Pergamon

Cement and Concrete Research, Vol. 26, No. 7, pp. 1029-1044, 1996

0008-8846/96 $15.00 + .00

PII S0008-8846(96)00090-7

MICROSTRUCTURAL AND MICROANALYTICAL STUDIES OF SULFATE ATTACK. V. COMPARISON OF DIFFERENT SLAG BLENDS

R.S. Gollop and H.F.W. Taylor
Blue Circle Industries PLC
Technical Centre, 305 London Road
Greenhithe, Kent DA9 9JQ, UK

(Refereed)
(Received February 23, 1996; in final form May 7, 1996)

ABSTRACT

Pastes of several slag blends that had been stored in 0.25 mol l^{-1} solutions of sodium or magnesium sulfate were studied by scanning electron microscopy using backscattered electron (BSE) imaging and X-ray microanalysis of polished sections. In general, attack resulted in decalcification of C-S-H and the formation of ettringite. With Na_2SO_4, little or no gypsum was formed, but with $MgSO_4$, brucite, poorly crystalline serpentine ($M_3S_2H_2$) and gypsum were also formed. Visual examinations and BSE images indicated that the relative susceptibility of the blends to attack by Na_2SO_4 increases with the content of Al_2O_3 available for the formation of ettringite; this includes that present in AFm phases but not that present in C-S-H or hydrotalcite. The rank order of susceptibility to attack by $MgSO_4$ was broadly similar to that by Na_2SO_4, but the slag blends performed more poorly relative to plain Portland cement or sulfate-resisting Portland cement. Resistance to attack by Na_2SO_4 is favoured by the use of high proportions of slag, slags low in Al_2O_3, or sulfate resisting Portland cements, and by supplementing the gypsum in the Portland cement component by additional calcium sulfate.

Introduction

In Part 4 of this series (1), we described the results of an investigation on a blend of a Portland cement (PC) with a blastfurnace slag. In this paper, we describe the results of parallel investigations on some other blends, which were selected in order to examine the effects of varying the composition or proportion of slag, especially in regard to its content of Al_2O_3, and of adding additional gypsum.

Locher (2) studied the resistance to attack by a sodium sulfate solution of a number of blends of Portland cement clinker and ground granulated blastfurnace slag (ggbs), to all of which 5% of gypsum had been added in order to simulate the factory production of Portland Blastfurnace Cement. The blends containing at least 65% of slag were highly resistant to attack, but with those containing less slag the resistance depended markedly on the Al_2O_3 content of the slag and the C_3A content of the PC. In general, blends containing up to about 50% of slag were less resistant than the plain PC if the slag was high in Al_2O_3 (18%) but more resistant if it was low

TABLE 1
Data for the Slags*

Slag	X	Y	Z
Type	Pelletised	Granulated	Granulated
Al_2O_3%	11.2	13.4	16.0
MgO%	7.7	8.3	11.0
S^{2-}%	0.97	0.82	1.1
Glass,%	89	100	100
Specific surface area†	397	395	384

* For full data, see references given in the text.
† Lea and Nurse; m^2kg^{-1}

in Al_2O_3 (11%). Kollek and Lumley (3), Osborne (4) and others have reported broadly similar results. Some investigators have reported that durability can be increased by supplementing the gypsum present in the Portland cement component with an appropriate proportion of additional calcium sulfate (3,5), but in one investigation no significant effect was found (6).

Starting Materials and Experimental Procedures

All the blends used in the present investigation were ones that Kollek and Lumley (3) had used in their durability study on mortars. The PC and slags have been described in their paper and elsewhere. The PC was their cement C and was also described in Part 1 (7). It was a normal Portland cement, low in alkalis (equivalent Na_2O 0.34%) and contained 2.3% of SO_3. The slags were slags Y and Z of Refs 3 and 8. The results will be compared with those described in Part 4 for a blend of the same PC with another slag, which was described as slag X in Refs 1, 3 and 8. The gypsum was a high purity commercial product containing over 96% of $CaSO_4{\cdot}2H_2O$.

TABLE 2
Compositions of Blends

Designation		Mass percentages			Total% of sulfur expressed as SO_3	Total percentage of sulfur present		Percentage of slag reacted at 6 months
Blend	Slag	Slag	PC	Gypsum		in SO_4^{2-}	as S^{2-}	
69X	X	69	31	0	0.8	0.3	0.7	33*
69Y	Y	69	31	0	0.7	0.3	0.6	39
69Z	Z	69	31	0	0.8	0.3	0.8	37
92Y	Y	92	8	0	0.2	0.1	0.8	27
65YG	Y	65	30	5	3.0	1.2	0.5	39

* 39% of the slag glass.

Blends were prepared as described in Ref. 1. Table 2 gives their com-positions, including that of the one (69X) described in that paper. It also includes data for the contents of SO_4^{2-} and S^{2-} and for the percentage of the slag that had reacted at an age of 6 months. Except in blend 65YG, much more sulfur is present as S^{2-} than as SO_4^{2-}. The percentages of slag reacted were obtained by interpolation (or for blend 69Z, extrapolation) from data reported by Lumley et al. (8), who used an EDTA extraction method.

Kollek and Lumley (3) found that mortars of w/s ratio 0.6 made with blends 69Y and 69Z had survival times of approximately 6 months when stored in 0.25 mol l^{-1} solutions of either Na_2SO_4 or $MgSO_4$. A mortar made with blend 69X was more durable, its survival time being somewhat over 1 year in each case. Compared with mortars made with the PC alone, all were more durable in Na_2SO_4 and either more durable (69X) or about equally durable (69Y and 69Z) in $MgSO_4$. Under other conditions, with a different ratio of slag to PC or in solutions of other sulfate concentrations, slag Z performed worse than slag Y. Mortars made with blend 65YG were highly durable in either Na_2SO_4 or $MgSO_4$. Those made using blend 92Y were highly durable in Na_2SO_4, but less so in $MgSO_4$, the survival times being 3 years and somewhat over 1 year, respectively.

Pastes were prepared at w/s = 0.3 and moulded into 25 mm cubes, which were stored at 20°C in 0.25 mol l^{-1} solutions of Na_2SO_4 or $MgSO_4$ for varying periods, the solutions being replaced after total periods of 3, 6, 12 and 24 months. Cubes were also stored in water for periods of up to 105 weeks. All the experimental procedures used in the preparation and examination of the samples have been fully described in previous papers in this series (1,7).

Results

Phase Compositions of Pastes Stored in Water. The samples were examined by XRD, and in some cases also by TG or DSC, at ages of 1-105 weeks. Except in the case of blend 65YG, the phases found were C-S-H, hydrotalcite (as defined in Ref. 1), an AFm phase or phases, minor amounts of CH and residual slag and clinker phases. Contents of CH, estimated using thermogravimetry, were typically around 2-3% referred to the ignited mass, or less for blend 92Y. CH was undetectable in the pattern from this blend after 105 weeks.

The most significant variations between the samples concerned the low-angle XRD peak attributed to the AFm phase. With blends 69Y and 69Z, this was relatively sharp and of spacing 0.88 nm at an age of 1 week, but with increasing age, up to 105 weeks, it gradually changed to an extremely weak and sometimes doubtful rise in the background, extending from about 0.9 nm to 1.1-1.2 nm. With blend 92Y, the peak took this form also at 1 week. The peak at 0.88 nm is attributed to an AFm phase approximating to monosulfate, though probably containing some S^{2-}. With increasing age, the relative contribution from the slag to the hydration products increases, causing the AFm phase to take up an increasing proportion of S^{2-} and to decrease in crystallinity or amount or both. With blend 65YG, a relatively sharp peak at 0.90 nm was observed at 1 week, which at later ages broadened into a diffuse band at 0.88-0.96 nm; in addition, peaks of ettringite were observed at all ages.

Peaks of a hydrotalcite-type phase were observed in all cases. They increased in intensity with time and were especially strong in the case of blend 69Z; this is consistent with the high MgO content of slag Z. Residues obtained by EDTA extractions (8) of 1 and 13 week old pastes of this blend gave a pattern which included the 7 strongest peaks of a hydrotalcite-type phase.

A least-squares refinement showed the hexagonal unit cell to have $a = 0.306$ nm, $c = 2.302$ nm. This is similar to what was found with blend 69X (1). The presence of this phase was also shown by DSC.

Pastes Stored in Sodium Sulfate Solution

Visual examination. Fig. 1 includes photographs of cubes of all the slag blends after 2 years' storage in the Na_2SO_4 solution and of cubes stored in water for comparison. Cubes of the plain PC (7) and of the sulfate-resisting Portland cement (SRPC; Ref. 9) are also included.

The cubes of blends 69Y and 69Z stored in Na_2SO_4 solution showed greater damage at any given age than those of the plain PC (7) or blend 69X (1). Cracks developed initially on the bottom surface and gradually extended to all surfaces; there was some swelling at the corners, which became rounded. Deposits of calcite, identified by XRD, formed on the surfaces. The approximate sequence of increasing damage shown in Fig. 1 is 69Z (most damaged) > 69Y > PC > 69X > SRPC > 92Y ≈ 65YG. With increasing time, the sequence did not change but the differences increased. After 4 years, the cubes of blend 69Z had partly disintegrated, but those of blends 92Y, 65YG and the SRPC were relatively little damaged.

Microstructures. Cubes of all the blends were examined in the SEM after 6 months' storage in the Na_2SO_4 solution, using backscattered electron (BSE) imaging and X-ray microanalysis of polished sections. Those of blends 69Y and 69Z showed layers of calcite, typically 10-15 μm thick, on the faces remote from the cube edges. Further in, for some 50-150 μm, there was a zone that appeared dark in the BSE image, suggesting decalcification. At the cube edges, there was extensive microcracking, especially in the case of blend 69Z, which showed a major crack extending inwards for some 2 mm. In contrast to what was observed with the plain PC (7) and with blend 69X (1), the other cracks at the cube edges were not preferentially oriented at right angles to the diagonal and no gypsum veins were observed beneath either the faces or the edges of the cube. However, in the cube of blend 69Y, a pore lined with gypsum was observed at a depth of approximately 400 μm inwards from the cube edge. At depths above about 2 mm, there were no apparent differences from the core materials, which had microstructures typical of normal slag cement pastes as reported, e.g., by Cao and Detwiler (10).

The cubes of blends 92Y and 65YG that had been stored in Na_2SO_4 solution showed much less damage than the above. On the cube faces, there were layers of calcite some 20 μm thick, below which were darkened layers up to 60 μm thick in the case of blend 65YG and up to 20 μm thick in that of blend 92Y. The microstructures at the cube edges were similar to those at the faces, and in neither case was there any significant cracking. At depths greater than those mentioned above, the microstructures appeared normal.

These results are consistent with those of the visual examination.

Microanalyses. As with blend 69X (1), microanalyses were made of the hydrated material in the core regions and of regions at various depths measured inwards perpendicular to a face or diagonally inwards from an edge of the cube. For each blend, the Si/Ca and S/Ca ratios were plotted against depth and for each region, atom ratio plots were made of Mg/Ca against Si/Ca and against Al/Ca, of (Al-Mg/2.0)/Ca against Si/Ca ("A-type" plots) and of S/Ca against (Al-Mg/2.0)/Ca ("B-type" plots).

Plots of Si/Ca and of S/Ca against depth. The plots of Si/Ca against depth gave little information that was not confirmed in greater detail by the A-type plots and will not be described.

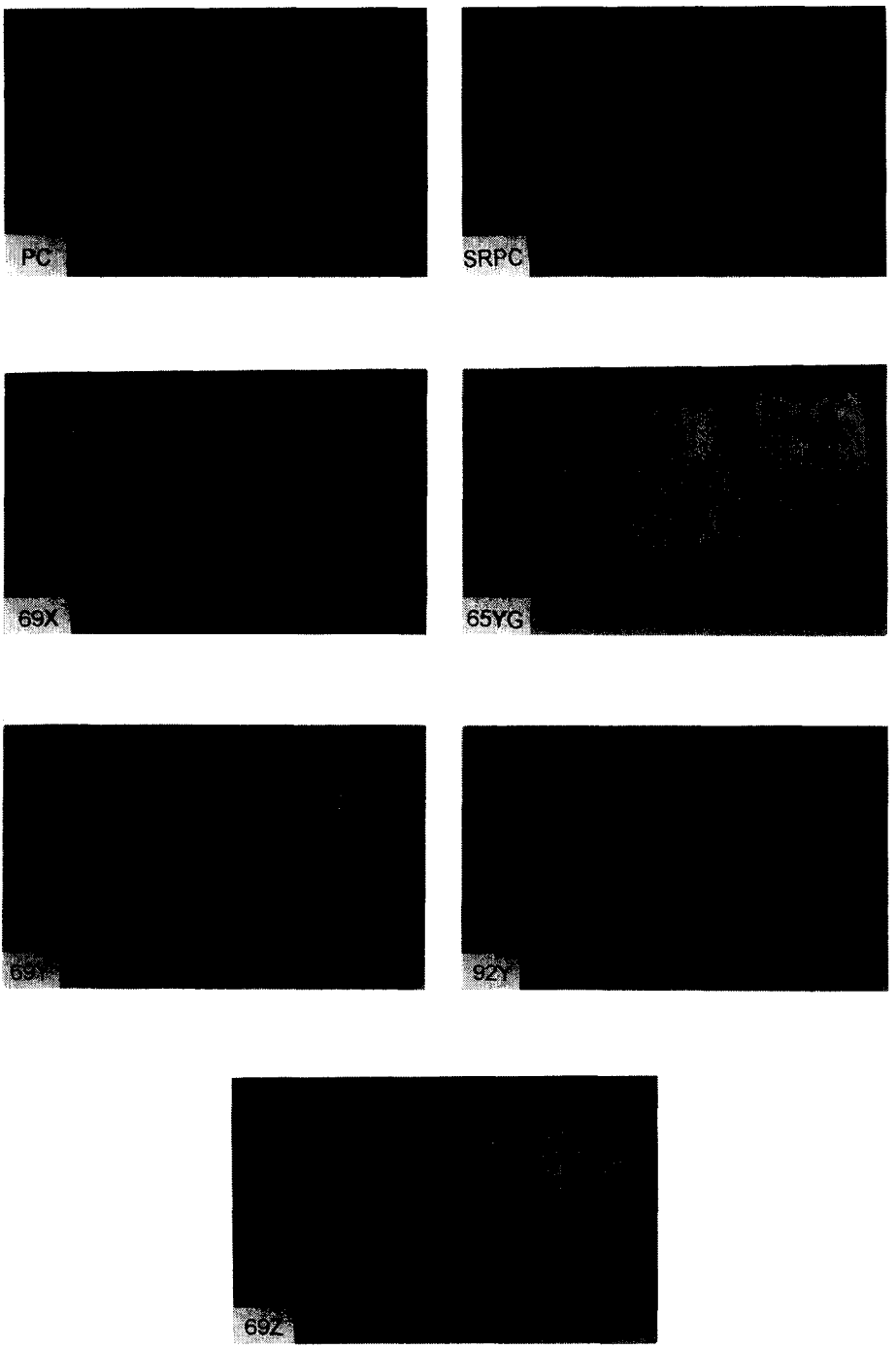

FIG. 1.
Photographs of cubes of pastes made from Portland cement (PC), sulfate-resisting Portland cement (SRPC) and various slag blends, after 2 years' storage in water or 0.25 mol l^{-1} sulfate solutions.

The S/Ca ratios in the core regions were in general very low, with a majority of values below 0.05. For blend 65YG, which was made with added gypsum, the values were higher, with a median of 0.10. In all cases, the S/Ca ratios tended to increase as the face or edge of the cube was approached. In a typical case, that of blend 69Y, the median value was 0.03 in the core and 0.13 at depths of 700-1200 μm below the edge of the cube. The depths below the cube faces at which the increases became significant varied from 500-600 μm for blends 92Y and 65YG to over 1000 μm for blends 69Y and 69Z; the sequence was at least approximately that of increasing visible damage. Incomplete data indicated that, below the cube edges, the corresponding depths were somewhat greater. A few spots of gypsum were recorded at depths of 200-400 μm below the face and edge in the case of blend 69Y, but none was found with blends 69Z, 92Y or 65YG. The increases in S/Ca ratio were often substantial at depths where those in Si/Ca ratio were slight or apparently non existent.

Plots of Mg/Ca against Al/Ca and against Si/Ca. As with blend 69X, the plots of Mg/Ca against Al/Ca, supported by those of Mg/Ca against Si/Ca, indicated that the hydrotalcite had a Mg/Al ratio of approximately 2.0 in all cases and that it was closely associated with the C-S-H. This allows the quantity (Al-Mg/2.0)/Ca to be used as a ratio in which Al present in hydrotalcite is excluded. This correction was first used by Wang and Scrivener (11). For blends 69Y and 69Z the plots showed that the Al/Ca ratio of the C-S-H was always close to 0.1. For blend 92Y, the Al/Ca ratio of the C-S-H was approximately 0.15. The plot for blend 65YG was anomalous and is described later.

A- and B-type plots: identification of hydrated phases and C-S-H composition. Except as noted subsequently, the A- and B-type plots for blends 69Y, 69Z and 92Y were similar in form to those for blend 69X (1). Based mainly on the data from these plots, the phases present in each region of each cube were determined. Table 3 gives the results, and includes indications of the distributions of Si/Ca ratios in the C-S-H. It was assumed that spots having a Si/Ca ratio between 0.6 and 1.2 consisted essentially of C-S-H and that those of higher Si/Ca ratios, described as strongly decalcified material, consisted wholly or partly of hydrous silica and alumina.

For blends 69Y and 69Z, the median values of the Si/Ca ratio for the C-S-H in the core material were 0.65 and 0.68, respectively. In agreement with the conclusion from the plots of Mg/Ca against Al/Ca, the Al/Ca ratio of the C-S-H was approximately 0.1. From the B-type plots, the S/Ca ratios were found to be approximately 0.03. Decalcification of the C-S-H and slight increases in its S/Ca ratio were apparent from depths of approximately 1 mm below either the face or edge of the cube. Except in the last 150-200 μm below the surface, it usually took the form of an upward trend in the Si/Ca ratio of the C-S-H rather than complete decomposition of that phase. It was somewhat greater for blend 69Z than for blend 69Y, notably at depths of 200-700 μm below the edge of the cube.

For blend 92Y, the median Si/Ca and Al/Ca ratios in the core material were 0.73 and 0.16, respectively (Table 3 and Fig. 2). These values are distinctly higher than those for blends 69Y or 69Z. The increases in both ratios with slag content are similar to those reported by Richardson and Groves (12). Decalcification of the C-S-H was barely significant at depths above 200 μm below the face or edge of the cube.

For blends 69Z and 92Y, occasional small regions of highly decalcified material were observed, even in the cores. These appeared to be inner product of either clinker, or more often, slag grains, and were abnormally high in alkalies relative not only to Ca but to other elements.

TABLE 3
Phases Detected by X-Ray Microanalyses of Cubes Stored in Na_2SO_4 Solution

Blend and Region	Number of analyses	Analyses with Si/Ca > 0.6				Phases detected*	
		Number	Median	% with Si/Ca greater than 0.8	1.2	Major	Minor or trace
Blend 69Y							
Core	36	19	0.65	0	0	C-S-H, X	CH
Face 700-950 μm	17	5	0.66	20	0	C-S-H, Mon	CH
Face 200-700 μm	29	9	0.67	11	0	C-S-H, Mon, Ett	CH, Gyp
Face < 200 μm	20	16	2	88	69	Decalc	C-S-H (?), Ett (?)
Edge 700–1200 μm	32	20	0.73	20	10	C-S-H, Mon	CH, Decalc
Edge 200–700 μm	37	19	0.70	32	5	C-S-H, Mon, Ett	Gyp, CH, Decalc
Edge < 200 μm	8	5	1.70	100	100	Decalc	Ett (?), $CaCO_3$
Blend 69Z							
Core	38	17	0.68	12	6	C-S-H, X	CH, Decalc.
Face 700–1100 μm	20	12	0.67	0	0	C-S-H, Mon	Ett, CH
Face 200–700 μm	25	12	0.70	17	0	C-S-H, Ett	CH, Mon
Face < 200 μm	19	15	1.54	63	60	Decalc	$CaCO_3$
Edge 700–1200 μm	40	15	0.66	13	0	C-SH, Mon, Ett	CH
Edge 200–700 μm	30	21	1.06	81	38	C-S-H, Ett, Decalc	Mon
Edge < 200 μm	11	11	1.74	100	91	Decalc	C-S-H (?)
Blend 92Y							
Core	38	31	0.73	29	6	C-S-H, X	Decalc.
Face 400–650 μm	18	13	0.74	0	0	C-S-H, Mon	
Face 200–400 μm	14	10	0.80	50	0	C-S-H, Mon	Ett (?)
Face < 200 μm	23	22	1.77	96	82	Decalc.	
Edge 700–1000 μm	17	13	0.74	23	0	C-S-H	Mon, Str (?)
Edge 200–700 μm	30	22	0.73	9	0	C-S-H, Mon	Ett (?)
Edge < 200 μm	11	7	0.99	86	29	Decalc	Ett (?)
Blend 65YG							
Core	56	31	0.66	0	0	C-S-H, Mon, Ett	CH
Face 700–1100 μm	16	9	0.65	0	0	C-S-H, Mon, Ett	CH
Face 200–700 μm	25	13	0.65	0	0	C-S-H, Ett, Mon	CH
Face < 200 μm	13	11	1.12	64	45	Decalc	Ett (?), C-S-H (?)
Edge 700–1200 μm	19	8	0.64	9	0	C-S-H, Mon, Ett	-
Edge 200–700 μm	37	12	0.66	8	0	C-S-H, Ett	Gyp
Edge < 200 μm	21	14	0.88	50	21	Decalc	Ett, C-S-H

* Phases other than hydrotalcite. Mon = AFm phase approximating to monosulfate; Str = strätlingite (C_2ASH_8); X = product of high Al/Ca and low S/Ca ratios (see text); Ett = ettringite; Gyp = gypsum; Decalc = strongly decalcified material high in SiO_2 and Al_2O_3 (Si/Ca > 1.2).

In other analyses, the ratios relative to Ca of elements other than Mg, Al, Si and S were with few exceptions low, except in the strongly decalcified material close below the faces or edges of the cubes. They were similar to those found with blend 69X (1).

Product "X", of high Al/Ca and low S/Ca ratios. For blend 69X, the Al-rich hydrated phase in the core material had Al/Ca and S/Ca ratios of 0.5 and 0.25, respectively, and thus approximated to monosulfate, though some of the sulfur could well have been present as sulfide (1). For blends 69Y, 69Z and 92Y, the microanalyses of the core regions showed the hydrated aluminate phase to be of higher Al/Ca and lower S/Ca ratio. It is illustrated in Fig. 2 and designated "X" in Table 3. Product X could be a mixture or intergrowth of monosulfate, or of a sulfide-containing AFm phase similar to monosulfate, with a phase higher in Al_2O_3 and lower in sulfur. The known possibilities are strätlingite (C_2ASH_8), C_2AH_8 and hydrogarnet. All have been reported, though extremely rarely, in pastes made from blastfurnace slag cements (13-16).

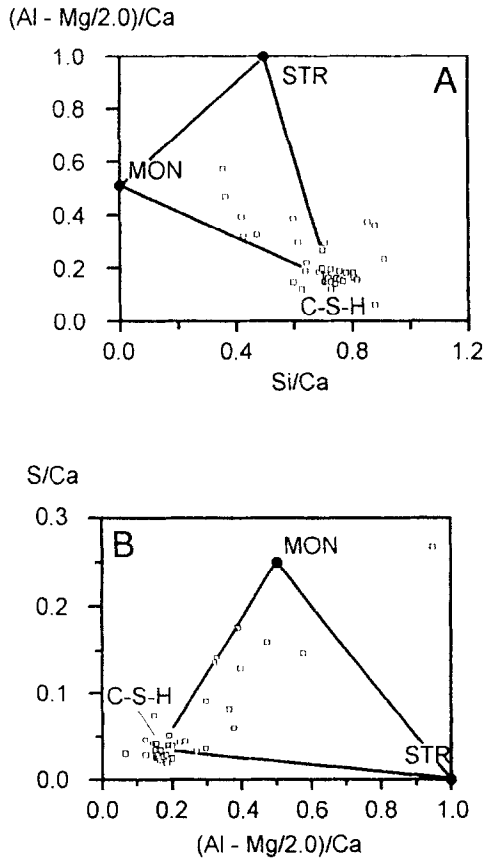

FIG. 2.
A-type and B-type atom ratio plots for the core region of the cube of blend 92Y stored in Na_2SO_4 solution. MON = AFm phase approximating to monosulfate; STR = strätlingite (C_2ASH_8).

Probably the most likely of these possibilities is strätlingite, which has been positively identified in a paste made with a gasifier slag containing 20% of Al_2O_3 (15). It was also identified by means of TEM microanalysis as a possible component of a mixture or intergrowth with monosulfate in a paste made using a normal granulated blastfurnace slag (16). A similar product might also account for the XRD evidence in the present case: at early ages, the hydration products come largely from the PC, and thus include an AFm phase approximating to monosulfate, but as the relative contribution from the Al-rich slag increases, this is supplemented by strätlingite. The formation of this phase in the two blends with the highest proportions of Al_2O_3 in the hydration products would be in accordance with its composition. Intimate interlayering of AFm phases might explain the broad and very weak XRD band shown by the older water cured pastes of most of the blends. This band extended approximately from the monosulfate peak at about 0.89 nm towards that of strätlingite at 1.26 nm.

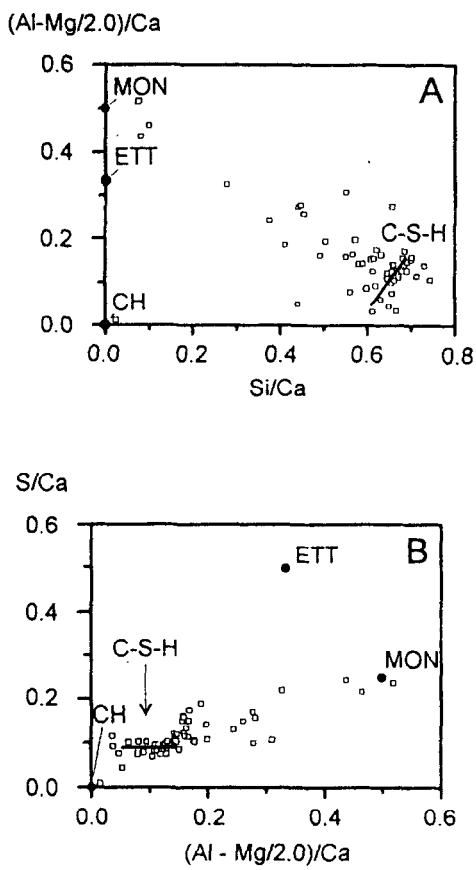

FIG. 3.
A-type and B-type atom ratio plots for the core region of the cube of blend 65YG stored in Na_2SO_4 solution. The lines indicate a possible range of C-S-H compositions. MON = AFm phase approximating to monosulfate; ETT = ettringite.

Changes affecting the Al-rich phases or calcium hydroxide. As the faces or edges of the cube were approached, Product X was replaced first by material approximating to monosulfate, then by ettringite and, finally, by strongly decalcified material (Table 3). In general, Product X had disappeared at depths of less than approximately 1 mm. The region at depths of 700-1000 μm below the edge of the cube of blend 92Y was a probable exception, showing 3 spots lying approximately on the compositional join between C-S-H and strätlingite. This provides some further support for the hypothesis that strätlingite is formed. Evidence of ettringite formation in the cube of blend 92Y was marginal. The small amounts of CH present in the core materials probably also decreased in all cases as the cube faces or edges were approached.

Effects of additional gypsum. A- and B-type plots for the core material of blend 65YG (Fig. 3 A and B) showed the presence of C-S-H, monosulfate, ettringite and a little CH. The ettringite was closely mixed with the C-S-H and its presence might have been undetected but for the unequivocal XRD evidence on the paste stored in water. Its presence was reasonably apparent in the B-type plot, but not in the A-type plot. This was probably due to the spread of composition in the C-S-H and the close mixing of the two phases.

The A- and B-type plots of the core material (Fig. 3) gave some indication of a range of C-S-H composition extending from Si/Ca 0.6, Al/Ca 0.03 to Si/Ca 0.7, Al/Ca 0.15, with S/Ca 0.09 in all cases. The plot of Mg/Ca against Al/Ca (Fig. 4) could be reconciled with this hypothesis. These observations might possibly be explained by the hypothesis that the C-S-H formed close to, or as inner product of the clinker grains has lower Si/Ca and Al/Ca ratios than that formed elsewhere in the structure. The median Si/Ca ratio of the C-S-H in the core material was 0.66 (Table 3).

As the face or edge of the cube was approached, the monosulfate was replaced by ettringite (Table 3). Decalcification of the C-S-H was insignificant at depths greater than 100 μm below

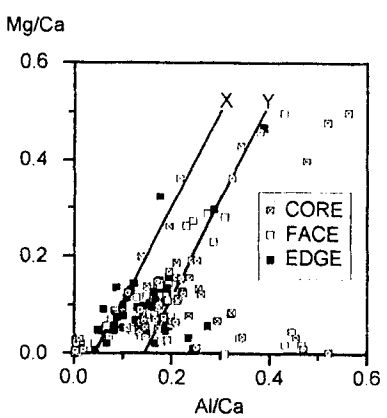

FIG. 4.

Atom ratio plot of Mg/Ca against Al/Ca for the cube of blend 65YG stored in Na_2SO_4 solution. The lines X and Y both have a slope of 2.0, which represents the Mg/Al ratio of the hydrotalcite, and make intercepts on the horizontal axis of 0.05 and 0.15, respectively, which may represent Al/Ca ratios of two types of C-S-H. Analyses within 200 μm of a face or edge are excluded.

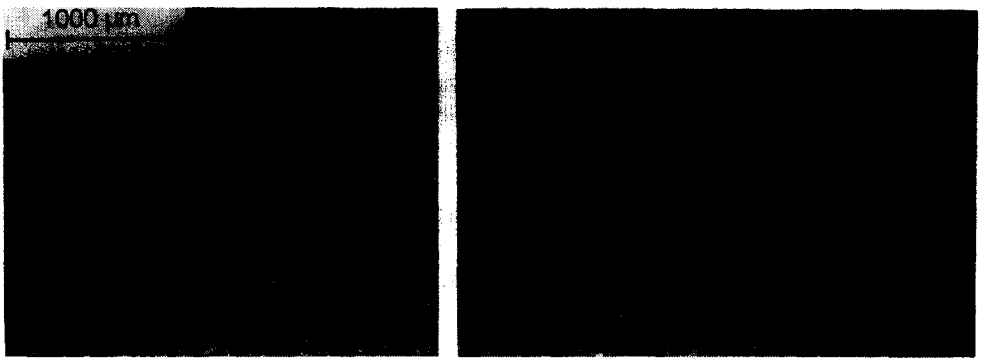

FIG. 5.
Backscattered electron image of a section of the cube of blend 92Y that had been stored in $MgSO_4$ solution and cut parallel to a cube face. A cube edge is shown at the top left hand corner.

the cube face or 200 µm below the cube edge. A single analysis of gypsum was recorded at a depth of 200 µm below the cube edge.

Cubes Stored in Magnesium Sulfate Solution

Visual examination. Fig. 1 includes photographs of cubes after storage for 2 years in the $MgSO_4$ solution. For any given blend, damage progressed much more quickly than in Na_2SO_4 solution. Damage took the form of swelling, spalling and rounding of corners, and the cubes became very weak. XRD showed little formation of brucite on the surfaces, but aragonite was often present. In contrast to what was found with Na_2SO_4 solution, the cubes of blend 92Y showed very marked swelling, rounding of corners and exfoliation. The sequence of increasing damage (Fig. 1) was, approximately, 69Z (most damaged) > 69Y > 92Y > 69X > PC > 65YG ≈ SRPC. This sequence differs from that for the cubes stored in Na_2SO_4 solution in that the plain PC and SRPC suffered less attack relative to the slag blends. By 4 years, the cube of blend 69Z had totally disintegrated.

Microstructures. Cubes of blends 92Y and 65YG that had been stored for 6 months in $MgSO_4$ solution were examined by BSE imaging and X-ray microanalysis. Both samples showed alteration both at the faces and the edges. For blend 92Y (Fig. 5), the material below the cube faces showed massive exfoliation with associated gypsum veins and darkened paste for depths of up to 1 mm; similar effects were observed at the cube edges at depths of up to 1.5 mm along the diagonal. For blend 65YG, the outermost 50 µm below the cube faces was very dark, and the next 50 µm moderately dark, with gypsum veins sub parallel to the surface. At the edges, the material was dark and extensively cracked in a region extending inwards for some 500 µm along the diagonal. Both in this region and further in, there were gypsum veins approximately perpendicular to the diagonal. The core region of the cube of blend 65YG had a porous appearance, unlike that of any of the other specimens examined, and possibly caused by polishing faults.

Microanalyses of Blend 65YG. Microanalyses of a region within 100 μm of the cube face showed the material to consist largely of brucite, strongly decalcified material and residual unreacted slag and clinker phases (mainly ferrite), together with an irregular vein of gypsum. The material within 500 μm of the cube edge, measured along the diagonal, consisted largely of magnesium silicate hydrate ($M_3S_2H_2$ approx; Refs 7 and 9) with some gypsum. X-ray microanalyses of other regions were considered unreliable and are not reported.

Microanalyses of Blend 92Y. The Si/Ca, S/Ca and Mg/Ca ratios all increased very sharply when the face of the cube was approached more nearly than about 800 μm. The increase in S/Ca began at a depth of about 1500 μm. Both in the core and at depths of 900-1200 μm below the cube face, plots of Mg/Ca against Al/Ca showed the presence of hydrotalcite with a Mg/Al ratio of 2.0 and C-S-H with an Al/Ca ratio of 0.15. The A-type and B-type plots for the core region were in moderate agreement with those for the cube stored in Na_2SO_4 solution, and thus showed the presence of C-S-H and Product X. At depths of 900-2000 μm below the face, Product X had been largely replaced by monosulfate, with some indication also of ettringite, and there was minor decalcification of the C-S-H.

The material at depths of less than 900 μm below the cube faces, or some 1500 μm below the cube edges, was high in Mg, Si and Al, with relatively little Ca or S. All the hydrated calcium-containing phases appear to have been decomposed, the Ca^{2+} being either leached out or entering the gypsum that is formed. In Fig. 6, the relative contents of Mg, Si and Al in the region below the cube face are plotted on a triangular diagram. This way of plotting microanalysis data has been used by Bonen and Diamond in cement hydration studies (17). At depths of 10-650 μm, the Al/Si ratios are mostly near that of the unhydrated blend. As the surface is approached, the Mg/Si and Mg/Al ratios gradually increase, until at depths of less than about 350 μm a limit is reached which lies near to the join Mg_3Si_2-Mg_2Al.

With plain PC or SRPC stored in $MgSO_4$ solution, a poorly crystalline form of serpentine, of composition $M_3S_2H_2$, is formed (7,9), and ratios on the join Mg_3Si_2-Mg_2Al could arise from

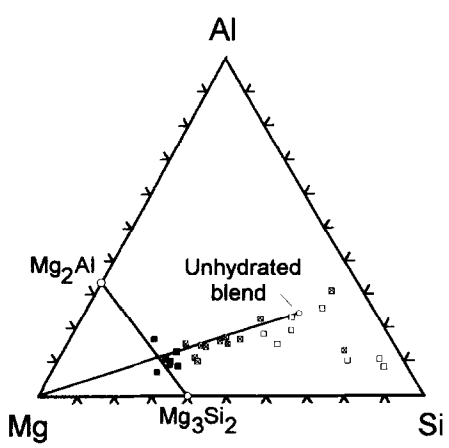

FIG. 6.
Triangular diagram showing the relative atomic contents of Mg, Si and Al in some regions of the cube of blend 92Y stored in $MgSO_4$ solution. Filled, shaded and open squares denote spots at depths below a cube face of 10-350 μm, 350-650 μm and 650-850 μm, respectively.

mixtures of this phase with hydrotalcite. An XRD examination confirmed this hypothesis. Some of the material that had spalled from the cube edge was extracted with water to remove the gypsum and examined by XRD. The pattern (CuKα radiation) showed sharp peaks corresponding to hydrotalcite and diffuse bands attributable to unreacted slag (26°-32° 2θ) and serpentine (20°-26°, 32°- 40°, 59°-63°, and possibly, overlapping the principal hydrotalcite peak, 10°-13° 2θ).

Concentrations of Ions in the Storage Solutions. For the Na_2SO_4 solution, the pH values were in the range 11.1-11.9 after 3 months and usually between 8.1 and 9.5 after 6-24 months, though in a few cases values of up to 11.6 were observed. For the $MgSO_4$ solution, they were 8.1-9.4 after 3 months and 7.3-8.3 after 6-24 months. These values are similar to those found with slag X (1). The Ca^{2+} and K^+ concentrations were mostly also similar to those found with slag X, though for blends 92Y and 65YG the K^+ concentrations after the first 3 months tended to be lower (e.g., 0.6-0.7 meqt l^{-1} in Na_2SO_4 solution, compared with 1.9 meqt l^{-1} for blend 69X).

Discussion

Effects of Slag Substitution on Resistance to Attack. Previous investigations at Blue Circle (3), supported by the visual examinations made in the present work, lead to the following conclusions regarding resistance to sulfate attack:

(i) Resistance to sulfate attack shown by a plain PC can be either increased or decreased through blending with slag. At high levels of substitution (e.g., 92%), resistance is always improved, often very substantially, but at low levels (e.g., 23%), it is little affected and may even be worsened.
(ii) For a given level of substitution, all other conditions being constant, resistance to attack increases with decreasing Al_2O_3 content of the slag.
(iii) Resistance can be substantially increased by including an appropriate quantity of gypsum in addition to that provided by the Portland cement constituent of a blend. This is the situation that normally prevails with factory produced Portland Blastfurnace Cements, which have typical SO_3 levels of ≈3%.
(iv) Resistance can also be substantially improved by specifying a sulfate-resisting Portland cement (SRPC).

These conclusions apply to attack by both Na_2SO_4 and $MgSO_4$ solutions, but with $MgSO_4$ the resistance is always lower than with Na_2SO_4. They agree substantially with those of Locher (2) and Osborne (8).

Damage associated with ettringite formation. Resistance to sulfate attack probably depends on several factors, of which the most important appears to be the quantity of Al_2O_3 that is available for the formation of ettringite. All the methods listed above for increasing resistance appear to be ones that decrease the amount of available Al_2O_3, or, more properly, of aluminate ions. Use of a slag lower in Al_2O_3 decreases the total quantity of aluminate ions released into the hydration products. Increased content of calcium sulfate in the blend causes some of the aluminate

to remain bound in ettringite from an early stage of hydration. The hydration products of an SRPC were found to contain very little available Al_2O_3 (9,18).

For typical slag compositions, between one-third and a half of the Al_2O_3 released by the slag is taken up in the hydrotalcite. The present results show that neither this, nor Al_2O_3 bound in the C-S-H, is readily available. The only substantial direct source of available Al_2O_3 appears to be the AFm phase or phases. Unreacted slag or clinker phases may be considered an indirect source of available Al_2O_3, effective to the extent that this is present in their respective hydration products.

It is not immediately obvious why high contents of a particular slag can improve the resistance whereas smaller contents can worsen it. Several factors may operate. One, recognised in part by Schröder and Smolczyk (14), lies in the differences in C-S-H composition. Richardson and Groves (12) showed that the amount of Al that can be accommodated in C-S-H, expressed as the Al/Ca ratio, increases with the Si/Ca ratio. At low contents of slag, the Si/Ca and Al/Ca ratios of the C-S-H do not differ greatly from those in the C-S-H of a plain PC. The higher contents of Al_2O_3 in slags, as compared with clinkers, may thus be reflected in larger amounts of Al_2O_3 available for the formation of ettringite. At high contents of slag, the Si/Ca and Al/Ca ratios of the C-S-H are considerably greater; the present results, in substantial agreement with those of Richardson and Groves (12), indicated values of 0.73 for Si/Ca and 0.16 for Al/Ca in the C-S-H of blend 92Y. Although more Al_2O_3 may be liberated from the anhydrous materials than at lower contents of slag, this could be outweighed by the greater amount taken up by the C-S-H.

Several other factors may enhance the ability of blends high in slag to resist damage associated with the formation of ettringite. One is the ability of the microstructure to accommodate an increase in solid volume without undergoing damage. We have discussed this in a previous paper (1); the effect, if real, would be expected to increase with the proportion of slag. A related effect arises because the proportion of slag that reacts under given conditions decreases with the content of slag in the blend (8). This limits the quantity of Al_2O_3 released and may also be presumed to increase the porosity, though it does not appear to affect the strength or the permeability. Yet another factor may be the permeability of the paste for sulfate ions. The present results showed a probable correlation between the depth of penetration and the extent of damage.

Damage Associated with Decalcification or Destruction of C-S-H. As we have previously noted (1), damage from sulfate attack can be attributed partly to ettringite formation and partly to reduction in the quantity of C-S-H through decalcification, or, with $MgSO_4$, total decomposition of this phase. The present results confirm that decalcification occurs with Na_2SO_4 as well as with $MgSO_4$ (Table 3). Decalcification in Na_2SO_4 was minimal with blends 92Y and 65YG, and increased in the sequence 69X (Ref. 1) < 69Y < 69Z, which is that of increasing damage. The low contents of CH in slag blends imply that the Ca^{2+} used in forming ettringite must come largely from decalcification of C-S-H. Ca^{2+} may also be consumed in the replacement of the alumina-rich constituent of "Product X" by monosulfate. The results confirm that, in $MgSO_4$, decalcification is much more marked, the C-S-H being completely destroyed in the regions in which attack has taken place. As with the PC, SRPC and blend 69X studied previously (1,7,9), it was accompanied by the formation of gypsum, brucite and poorly crystalline serpentine (M-S-H). A notable feature in the case of blend 92Y was the greater tendency to form M-S-H rather than brucite. This possibly reflects the high degree of attack and high content of SiO_2 in the blend.

The greater degree of attack produced by $MgSO_4$ as compared with Na_2SO_4 shows that the reactions involving Mg^{2+} are especially destructive. These reactions do not involve the aluminate ions. However, with the exception of 92Y, the sequences of increasing damage observed with $MgSO_4$ in this investigation, and by Kollek and Lumley (3), were broadly similar to those observed with Na_2SO_4, and in the latter case are associated with ettringite formation. It follows that ettringite formation must contribute significantly to the damage produced by $MgSO_4$.

Conclusions

1. For all the slag blends studied, storage of pastes in 0.25 mol l^{-1} Na_2SO_4 solution resulted to varying extents in the formation of ettringite and decalcification of C-S-H. The quantity of Al_2O_3 available for forming ettringite is considered to be a major factor affecting resistance to attack. In this context, available Al_2O_3 is primarily that present in AFm phases.
2. High resistance to attack by the Na_2SO_4 solution shown by a blend containing 92% of slag could be attributed mainly to a decrease in the quantity of available Al_2O_3 resulting from the greater uptake of this component by the C-S-H. Microstructural features and the relatively small degree of reaction of the slag may also have contributed to the high resistance.
3. High resistance of a blend containing 65% of slag that was obtained by including 5% of gypsum in addition to that supplied by the Portland cement could be attributed to the formation and retention of ettringite formed at an early stage of hydration, before sulfate attack had begun.
4. For blends containing 69% of slag, decreasing resistance with increase in the Al_2O_3 content of the slag could be attributed to increase in the quantity of available Al_2O_3. Reports that blending with a small proportion of slag high in Al_2O_3 can decrease resistance can be similarly explained.
5. The same reactions occurred with $MgSO_4$ solution as with Na_2SO_4 solution, but were accompanied by especially damaging ones leading to complete destruction of C-S-H and formation of poorly crystalline serpentine (a magnesium silicate hydrate), brucite and gypsum. The ranking order of damage from $MgSO_4$ for the various blends was broadly similar to that from Na_2SO_4, but the slag blends tended to perform more poorly relative to a PC or SRPC. The blend containing 92% of slag, which was highly resistant in Na_2SO_4, was strongly attacked in $MgSO_4$.
6. The AFm phase formed in slag blends at early stages of reaction approximates to monosulfate. Subsequently, it can decrease in crystallinity or quantity or both and probably takes up most of the sulfide ion released from the slag. In the case of blends high in slag, or made using slags of moderate or high Al_2O_3 content, the AFm phase appears to include strätlingite, which is intimately mixed with the sulfate or sulfide containing constituent.

Acknowledgements

The authors wish to thank Blue Circle Industries PLC for permission to publish this study and for sponsoring RSG for an External Ph.D. course at Imperial College, University of London. The work forms part of the programme of research being carried out by RSG under the Public

Institutions and Industrial Research Laboratories Scheme at Imperial College, where HFWT is a Visiting Professor. The authors are indebted to Dr G.K. Moir for his encouragement and advice. Similar thanks are due to the late Professor P.L. Pratt and to Dr K.L. Scrivener, of the Department of Materials, Imperial College. The authors also thank the following colleagues at the Technical Centre for assistance of various kinds: M.J. Coole, M.W. Duggan, P.V. Huggett and the late A.C. Sass.

References

1. R.S. Gollop and H.F.W.Taylor, Cem. Concr. Res. **26**, xxx (1996).
2. F.W. Locher, Zem.-Kalk-Gips **19**, 395 (1966). 3.J.J Kollek and J.S. Lumley, in Proc. 5th Int. Conf. Durability of Building Materials and Components (Ed. J.M. Baker, P.J. Nixon, A.J. Majumdar and H. Davies), p. 409. E & FN Spon, London (1991).
4. G.J. Osborne, in 2nd CANMET/ACI International Conference on Durability of Concrete (Montreal, 1991; Ed. V.M. Malhotra), Vol. 2, p. 1047. Special Publication SP 126, American Concrete Institute, Detroit (1991).
5. R. Kondo, in Chemistry of Cement. Proc. 4th Int. Symp. (Washington, 1960), Vol. 2, p. 881. N.B.S Monograph 43, US Department of Commerce, Washington (1962).
6. G. Frigione, in Blended Cements (Ed. G. Frohnsdorff), p. 15. ASTM Special Technical Publication 897, Philadelphia (1986).
7. R.S. Gollop and H.F.W. Taylor, Cem. Concr. Res. **22**, 1027 (1992).
8. J.S. Lumley, R.S. Gollop, G.K. Moir and H.F.W. Taylor, Cem. Concr. Res. **26**, 139 (1996).
9. R.S. Gollop and H.F.W. Taylor, Cem. Concr. Res. **25**, 1581 (1995).
10. Y. Cao and R.J. Detwiler, Cem. Concr. Res. **25**, 627 (1995).
11. S.D. Wang and K.L. Scrivener, Cem. Concr. Res. **25**, 561 (1995).
12 I.G. Richardson and G.W. Groves, J. Mater. Sci. **27**, 6204 (1992).
13. H.-G. Smolczyk, Zem.-Kalk-Gips **18**, 238 (1965).
14. F. Schröder and H.-G. Smolczyk, in F. Schröder, Proc. 5th Int. Symp. Chemistry of Cement (Tokyo, 1968), Vol. 4, p. 149. Cement Association of Japan, Tokyo (1969).
15. C.H. Bland, J.H. Sharp and A.P. Barker, Adv. Cem. Res. **4**, 159 (1991/1992).
16. I.G. Richardson, A.R. Brough, G.W. Groves and C.M. Dobson, Cem. Concr. Res. **24**, 813 (1994).
17. D. Bonen and S. Diamond, J. Am. Ceram. Soc. **77**, 1875 (1994).
18. R.S. Gollop and H.F.W. Taylor, Cem. Concr. Res. **24**, 1347 (1994).